Direct Measurement of Hyperfine Shifts and Radio Frequency Manipulation of Nuclear Spins in Individual CdTe/ZnTe Quantum Dots

G. Ragunathan,[1,*] J. Kobak,[1,2,†] G. Gillard,[1] W. Pacuski,[2] K. Sobczak,[3]
J. Borysiuk,[2] M. S. Skolnick,[1] and E. A. Chekhovich[1,‡]
[1]*Department of Physics and Astronomy, University of Sheffield, Sheffield S3 7RH, United Kingdom*
[2]*Institute of Experimental Physics, Faculty of Physics, University of Warsaw, ul. Pasteura 5, 02-093 Warsaw, Poland*
[3]*Biological and Chemical Research Centre, Faculty of Chemistry, University of Warsaw, ul. Żwirki i Wigury 101, 02-089 Warsaw, Poland*

(Received 27 September 2018; revised manuscript received 13 January 2019; published 7 March 2019)

We achieve direct detection of electron hyperfine shifts in individual CdTe/ZnTe quantum dots. For the previously inaccessible regime of strong magnetic fields $B_z \gtrsim 0.1$ T, we demonstrate robust polarization of a few-hundred-particle nuclear spin bath, with an optical initialization time of ∼1 ms and polarization lifetime exceeding ∼1 s. Nuclear magnetic resonance spectroscopy of individual dots reveals strong electron-nuclear interactions characterized by Knight fields $|B_e| \gtrsim 50$ mT, an order of magnitude stronger than in III–V semiconductor quantum dots. Our studies confirm II–VI semiconductor quantum dots as a promising platform for hybrid electron-nuclear spin qubit registers, combining the excellent optical properties comparable to III–V dots and the dilute nuclear spin environment similar to group-IV semiconductors.

DOI: 10.1103/PhysRevLett.122.096801

Proposed designs for solid-state quantum information processing devices require two essential components: the quantum nodes for storing and processing information and the quantum channels between them [1]. Various material systems using spin qubits as nodes and single photons as channels have been considered. Quantum dots (QDs) in group-III–V compound semiconductors are of particular interest, since they benefit from mature epitaxial technologies and exceptional single-photon properties [2–4]. However, the electron spin qubits [5] suffer fast decoherence due to the interaction with a dense nuclear spin environment [6,7]. By contrast, group-IV semiconductors, such as silicon and diamond, where most nuclei are spin-free, offer defect spin qubits with record coherence [8,9], whereas their optical properties are inherently limited. The advantages of the two approaches can be combined if optically active quantum dots can be grown of materials with spin-free nuclei. The II–VI semiconductors are a natural choice for this since most nuclei are spin-free and the direct band-gap character offers a good interface between electron spin and photons.

The research of the past two decades has lead to an in-depth understanding and development of advanced techniques for probing and manipulation of the nanoscale nuclear spin ensembles in III–V QDs [6,7]. By contrast, current understanding of the nuclear spin phenomena in II–VI dots is scarce, due to the challenges arising from the small nuclear spin magnetization in a dilute spin bath. Previous studies [10–13] relied on indirect detection of the nuclear spin effects via probing of the electron spin dynamics. Consequently, these experiments were restricted to low magnetic fields ($B \lesssim 0.1$ T), leaving beyond reach the most interesting regime where nonsecular electron-nuclear spin interactions are suppressed by the magnetic field giving access to long-lived electron and nuclear spin states, required for qubit applications.

Here we study high-quality CdTe/ZnTe structures and achieve direct detection of the hyperfine shifts in photoluminescence of individual quantum dots, giving access to nuclear spin phenomena in a wide range of magnetic fields. A cascade relaxation process via intermediate quantum well (QW) states is identified as a mechanism of efficient dynamic nuclear polarization (DNP) in magnetic fields up to 8 T. The DNP can be induced within ∼1 ms and persists in the dark over ∼1 s, 3 orders of magnitude longer than observed previously in II–VI QDs at low fields [11]. While in previous studies nuclear species could not be addressed individually, here we measure cadmium and tellurium nuclear magnetic resonance (NMR) signals in individual CdTe dots and observe strong electron-nuclear interaction characterized by Knight fields exceeding 50 mT. Our results suggest CdTe/ZnTe quantum dots as a promising system with the potential to implement a hybrid quantum spin register architecture [14], based on one electron coupled to several individually addressable nuclei, and with high optical efficiency unachievable in group-IV semiconductors.

We study two samples grown by molecular beam epitaxy. In sample *A*, low-density QDs are formed using the amorphous Te technique [15,16], whereas in sample *B*,

amorphous Te deposition is avoided, resulting in a higher QD density and preservation of the CdTe wetting layer QW (for further details, see Supplemental Material [17], Notes 1 and 2). Photoluminescence (PL) experiments are conducted at a temperature of 4.2 K with an external magnetic field B_z applied along the sample growth axis (Faraday geometry). PL of individual QDs is excited nonresonantly at 532 or 561 nm, and the emission is analyzed by a spectrometer and a charge-coupled device detector. Pump-probe measurements are implemented by modulating the PL signal and the laser polarization and power.

Figure 1(a) shows a broad-range PL spectrum of sample B exhibiting sharp spectral lines characteristic of QDs with full width at half maximum as low as 20 μeV. A strong, broad PL peak at ~2.15 eV is the QW emission. In most studied individual QDs, PL is dominated by recombination of a bright neutral exciton (X^0), recognized through its fine structure splitting at $B_z = 0$. In an external magnetic field B_z, X^0 becomes a doublet of states with electron spin parallel or antiparallel to B_z and with Zeeman energy splitting E_Z. Nuclear spins polarized along the z axis couple to the electron spin via the hyperfine interaction resulting in variation of E_Z [6,7]. Excitation with σ^+ or σ^- circularly polarized light repeatedly injects spin polarized electrons into the dot, leading to dynamic polarization of the nuclei via hyperfine interaction. The resulting change in splitting $|E_Z^{\sigma^-} - E_Z^{\sigma^+}|/2$ gives a lower estimate of the maximum electron hyperfine shifts. In III–V QDs, hyperfine shifts exceed 100 μeV, making it a pronounced effect [6,7,33].

Using the same approach, we investigate the effect of $\sigma^{+/-}$ excitation on PL spectra of CdTe/ZnTe QDs. We use a pump-probe scheme with the timing of Fig. 1(c): the pump pulse has a variable degree of circular polarization (e.g., σ^+, σ^-, or linear), while the PL is detected only during a short linear polarized probe pulse. Crucially, E_Z in a pump-probe scheme depends only on those effects of the pump that persist over a sufficiently long time T_{wait}, as should be the case for nuclear spin polarization. A typical result for sample B is presented in Fig. 1(b). The variation $(E_Z^{\sigma^-} - E_Z^{\sigma^+})/2 \approx 2$ μeV is smaller than the PL linewidths (36 μeV), but is detected reliably from Gaussian line shape fitting. Similar results are obtained from the measurements on ~20 individual QDs. The systematic nature and the sign (see Supplemental Material [17], Note 5) of the shift suggest DNP as its origin. By contrast, we find no DNP in sample A (without the QW). Thus, in what follows we present the data for sample B, while the additional results for sample A are discussed in the Supplemental Material, Note 3.

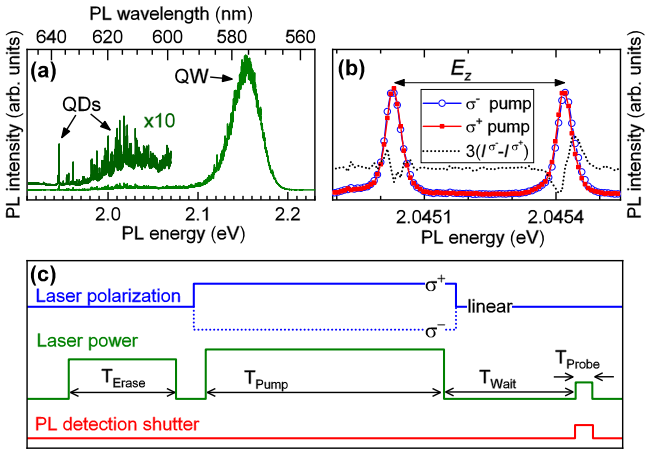

FIG. 1. (a) Broad-range PL spectrum from CdTe/ZnTe sample B. (b) Pump-probe PL spectra of X^0 in a QD measured at $B_z = 2.5$ T under σ^- (circles) and σ^+ (squares) polarized 561 nm pump laser: the change in splitting $(E_Z^{\sigma^-} - E_Z^{\sigma^+})/2 \approx 2$ μeV is revealed in the difference spectrum (dotted line, ×3 scaled for clarity) and gives a lower estimate of the maximum hyperfine shift. (c) Timing of the pump-probe measurement cycle. The erase pulse is used only in the buildup dynamics measurements [Fig. 2(c)].

Further investigation of DNP is presented in Fig. 2(a) where power dependent measurements are shown: at low power, E_Z (squares) does not depend on polarization of the pump, but at higher power, a clear increase (decrease) in E_Z is observed under σ^- (σ^+) pumping, saturating above ~50 μW, which coincides with the saturation of the X^0 PL intensity (triangles). Such saturation is observed in all studied dots in sample B and is in contrast to the III–V QDs where DNP under nonresonant optical excitation is often most efficient at optical powers significantly exceeding the ground state PL saturation [34–36], due to the role of multiexciton and excited QD states in DNP.

Figure 2(b) shows magnetic field dependence of $(E_Z^{\sigma^-} - E_Z^{\sigma^+})/2$: DNP is nearly absent at $B_z = 0$, reaching a maximum at $B_z \approx 2.5$ T. The lack of DNP at $B_z = 0$ T is due to the fine structure splitting ($\delta_b \approx 115$ μeV for this dot) resulting in zero electron spin polarization of the X^0 eigenstates, preventing interaction with nuclear spins [33]. With the applied magnetic field, $|E_Z|$ increases (at ≈150 μeV/T for this dot, see Supplemental Material [17], Note 4) restoring electron spin polarization of X^0 and enabling interaction with the nuclei. Significant DNP is observed up to $B_z = 8$ T; the partial reduction of DNP above 2.5 T is similar to that observed in III–V QDs [37] and is likely due to the mismatch in the electron and nuclear spin energy splitting, which increases with magnetic field, slowing down the DNP.

To understand the mechanism of DNP, we first note that in both samples circularly polarized light generates spin polarized excitons efficiently (Supplemental Material [17], Note 3), whereas DNP is observed only in sample B. This rules out DNP via electron-nuclear interaction during the ground-state exciton radiative lifetime or recombination. On the other hand, DNP reaching maximum with saturation of X^0 PL intensity and the suppression of DNP due to the fine structure splitting point to the key role of X^0 states. These two observations suggest that DNP occurs via a cascade relaxation of the electron-hole pair, where the

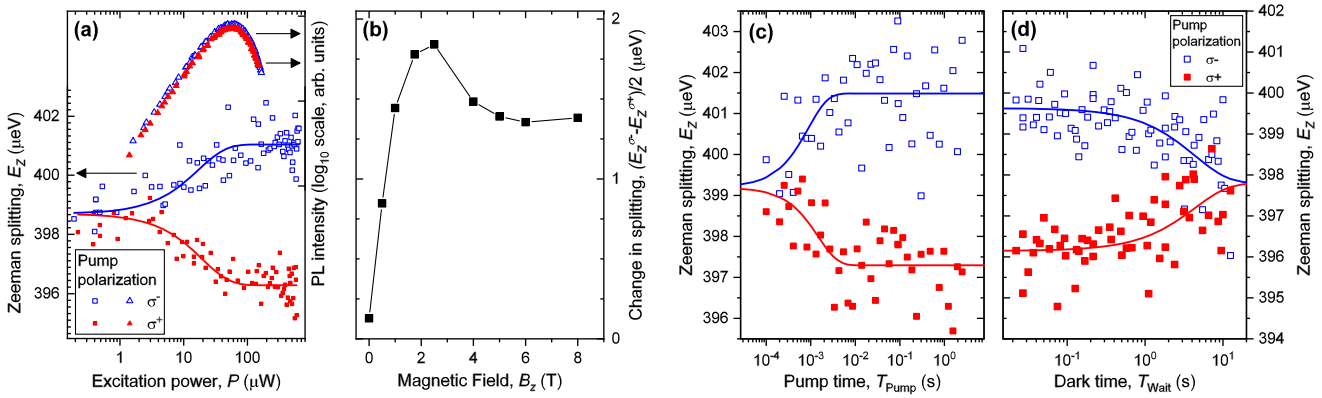

FIG. 2. (a) Total X^0 PL intensity of a QD from sample B measured as a function of continuous wave laser power (triangles, right scale), and Zeeman splitting E_Z measured in the pump-probe scheme (squares, left scale) as a function of pump power under σ^- (open symbols) and σ^+ (solid symbols) 561 nm laser excitation at $B_z = 2.5$ T. Lines show exponential fitting $E_Z(P) = E_Z(0) + \Delta E_Z[1 - \exp(-P/P_0)]$ with characteristic saturation power $P_0 \approx 18$ μW and saturated hyperfine shifts $\Delta E_Z^{\sigma^-} \approx 2.3$, $\Delta E_Z^{\sigma^+} \approx -2.4$ μeV. (b) Magnetic field dependence of the change in Zeeman splitting $(E_Z^{\sigma^-} - E_Z^{\sigma^+})/2$ measured in the pump-probe scheme. (c) Buildup dynamics of the optically induced nuclear spin polarization at $B_z = 2.5$ T. Symbols show experiment and lines show exponential fitting yielding 95% confidence estimates: $\tau_{\text{buildup}} = 0.9^{+1.3}_{-0.5}$ ms ($1.5^{+3.0}_{-1.0}$ ms) for σ^- (σ^+) polarized pump. (d) Decay of the nuclear spin polarization in the dark (symbols) in the same QD as in (a)–(c) and the exponential fit (lines) revealing the relaxation time $\tau_{\text{decay}} = 4.3^{+2.5}_{-1.6}$ s (95% confidence).

quantum well (present only in sample B) serves as an intermediate state and X^0 is the final state. Intermediate states with short lifetimes (and hence large energy broadening) facilitate the DNP by relaxing the energy conservation restriction on the electron-nuclear spin flip-flops [38].

We now investigate the nuclear spin dynamics in CdTe/ZnTe QDs. Open (solid) symbols in Fig. 2(c) show the buildup dynamics of the DNP under σ^- (σ^+) pumping, revealing characteristic buildup time $\tau_{\text{buildup}} \sim 1$ ms. Similar τ_{buildup} are observed on several individual CdTe QDs at $B_z = 2.5$ T and are a factor of ~1000 smaller than $\tau_{\text{buildup}} \sim 0.5$–3 s found in III–V QDs at similar magnetic fields [36,37,39,40]. DNP is expected to be a factor of ~30 faster in CdTe simply due to the lower spin ($I = 1/2$ vs $I = 3/2$ for Ga, As and $I = 9/2$ for In) and abundance (~25% for Cd and ~8% for Te, vs 100% for III–V). The remaining difference is attributed to a smaller number of atoms $\sim 5 \times 10^3$ estimated from transmission electron microscopy (see Supplemental Material [17], Note 1), as opposed to 10^4–10^5 atoms in typical III–V QDs. Our $\tau_{\text{buildup}} \sim 1$ ms measured at $B_z = 2.5$ T is an order of magnitude longer than $\tau_{\text{buildup}} < 100$ μs reported previously in CdTe/ZnTe [13] and CdSe/ZnSe [10] dots at low fields $B \lesssim 0.1$ T, which is well explained by the reduction of the electron-nuclear spin flip-flop probability due to the increasing mismatch in the Zeeman energies.

Measurements of the nuclear spin polarization dynamics in the dark are shown in Fig. 2(d), revealing a characteristic decay time $\tau_{\text{decay}} \sim 4$ s. Similar τ_{decay} are found in several CdTe QDs and are at least 3 orders of magnitude longer than submillisecond τ_{decay} reported for charged CdSe QDs at low magnetic fields [11], but are noticeably shorter than $\tau_{\text{decay}} \sim 10^2$–$10^5$ s observed both in neutral [37,39] and charged [41,42] III–V QDs at high magnetic fields. The long τ_{decay} in III–V QDs is due to the inhibition of spin diffusion by strain-induced quadrupolar effects, which are absent in CdTe. The expected diffusion time (Supplemental Material [17], Note 7) matches the observed τ_{decay} within an order of magnitude. Additional nuclear spin relaxation may arise from hyperfine interaction [41,42] with fluctuating charges intermittently occupying the dot [37] or nearby charge traps. Such charge fluctuations are evidenced in random spectral wandering of the PL energy (see Supplemental Material [17], Note 6) and are corroborated by NMR spectroscopy as shown below.

While optical methods can be used to initialize and probe the nuclear spin state, its complete control requires radio frequency (rf) magnetic fields. Figure 3 shows NMR spectra, obtained by depolarizing the nuclei at a variable rf frequency f_{rf}. In order to balance NMR spectral resolution and signal amplitude, the rf signal has the shape of a rectangular spectral band centered at f_{rf}. For ^{111}Cd the signal is amplified by simultaneous excitation of ^{113}Cd (see details in Supplemental Material [17], Note 8). Measurement on QD1 [Fig. 3(a)] show resolution limited negative peaks at ~22.6 and ~33.7 MHz, corresponding to the expected resonance frequencies of ^{111}Cd and ^{125}Te at $B_z \approx 2.5$ T.

From the NMR peak amplitude, the combined hyperfine shift of ^{111}Cd and ^{113}Cd is $|\Delta E_Z^{^{111}\text{Cd}} + \Delta E_Z^{^{113}\text{Cd}}| \approx 0.8$ μeV. The partial hyperfine shift of each isotope i is $\Delta E_Z^i = k^i \rho^i A^i I^i P_N^i$, where A^i is the hyperfine constant, P_N^i is the average nuclear spin polarization degree, ρ^i is the natural isotope abundance, and $0 \le k^i \le 1$ is the element mole fraction within the electron envelope wave function volume [6,7,13,33,42–44]. Using the bulk CdTe Knight

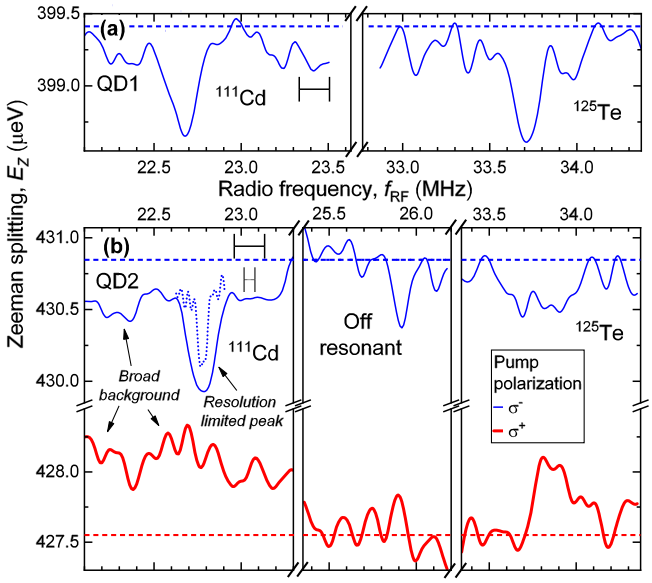

FIG. 3. Optically detected NMR spectra in individual CdTe/ZnTe quantum dots (a) QD1 and (b) QD2 in sample B at $B_z \approx 2.5$ T. Optical pumping is either σ^- (thin blue lines) or σ^+ polarized (thick red lines). The rf excitation depolarizing the nuclei has a rectangular-band spectrum with a width of 63 (dotted line) or 174 kHz (solid lines), which determines spectral resolution (also shown by the horizontal bars). Dashed horizontal lines show E_Z measured without rf.

shifts [45], we find $A^{^{111}\mathrm{Cd}} \approx -31$ μeV, $A^{^{113}\mathrm{Cd}} \approx -32$ μeV, and $\rho^i A^i I^i \approx -2.0$ μeV for either of the Cd isotopes. Applying linear interpolation to the bulk band gaps $E_0^{\mathrm{CdTe}} = 1.60$, $E_0^{\mathrm{ZnTe}} = 2.38$ eV, and the CdTe/ZnTe QD PL energy ≈2.05 eV, we roughly estimate for cadmium $k \approx 0.4$ and, consequently, $|P_N| \approx 0.5$. There is no experimental data for $A^{^{125}\mathrm{Te}}$, but we can expect that P_N is similar for all $I = 1/2$ isotopes (i.e., $|P_N| \approx 0.5$ for Te) as it is the case in GaAs/AlGaAs QDs [44]. Given the typical measured total hyperfine shift $\Delta E_Z \approx \pm 2$ μeV (Fig. 2), we estimate the maximum total shift ± 4 μeV (at $|P_N| = 1$) for the studied CdTe dots.

Similar NMR measurements on another individual dot [QD2, Fig. 3(b)] show a more complex picture. A clear peaklike structure is observed only for the measurement on Cd nuclei (~22.2–23.3 MHz) with σ^- pumping. Measurement with 174 kHz resolution (solid line) shows a combination of a resolution limited negative peak (~ -0.5 μeV amplitude) and a flat background offset of ~ -0.3 μeV with respect to the Zeeman splitting measured without rf (horizontal dashed line). Additional measurements with rf detuned from all isotopes [~25.4–26.2 MHz frequency range, Fig. 3(b)] reveal no systematic change in E_Z, confirming that the broad ($> \pm 0.5$ MHz width) background offsets observed for Cd in QD2 are real NMR signals and are not related, e.g., to rf-induced sample heating.

The spin-1/2 nuclei have no electric quadrupolar moments, while the nuclear-nuclear dipolar interactions are limited to few kilohertz. This leaves the inhomogeneous hyperfine (Knight) field B_e of the electron spin, acting on the nuclei of the dot as the only source of the broad background in the NMR spectra. The Knight shift of ^{111}Cd is $\gamma_{^{111}\mathrm{Cd}} B_e/(2\pi)$ (where $\gamma_{^{111}\mathrm{Cd}}$ is the nuclear gyromagnetic ratio) [13,43,46]. The observed shifts are at least ± 0.5 MHz in QD2, leading to the estimate of the maximum Knight field $|B_e| \gtrsim 50$ mT, a factor of ~5 larger than $|B_e| \sim 10$ mT observed in InGaAs [43] and InP QDs [37]. Such a large $|B_e|$ in CdTe QDs can be generated by electrons intermittently occupying the dot during rf excitation in the dark. The time-averaged NMR spectrum of ^{111}Cd under σ^- pump [Fig. 3(b)] is then explained as a sum of the narrow peak arising from an empty dot and a broad offset arising from the electron-charged state.

In the charged state, the average Knight shift of ^{111}Cd induced by a polarized electron with spin $s = 1/2$ can be estimated as $\sim sI|A^{^{111}\mathrm{Cd}}|/N \approx 3$ neV $\approx h \times 0.75$ MHz, where h is the Planck constant and $N \approx 2500$ is the number of group-II atoms within the electron volume. This estimate is close to the observed shifts ± 0.5 MHz, signifying that the correlation time of the resident electron spin is significantly longer than the nuclear spin precession period ($= 1/f_{\mathrm{rf}} \approx 40$ ns): at each point in time, the nuclei interact with a spin-up (spin-down) electron producing a Knight field $+|B_e|$ ($-|B_e|$) and giving rise to a signal on the high- (low-)frequency side of the NMR peak. In a time-averaged NMR spectrum, these signals add up and appear as a broad background due to the spatial inhomogeneity of the Knight field (nuclei in the center of the QD couple stronger to the electron) [47].

Having established the origin of the broad background, we examine the resolution limited NMR peak. A further measurement of ^{111}Cd NMR with a resolution of 63 kHz [dotted line in Fig. 3(b)] also yields a broad background offset and a resolution limited peak of reduced amplitude. Measurements with even better resolution result in a peak amplitude too small to detect, suggesting that the resolution limited peak itself consists of a narrow peak (width $\lesssim$63 kHz) and broader (~100 kHz) wings. The width of the wings again implies the Knight field as the cause, but unlike the wide background, this smaller broadening is likely to arise from the Knight fields of the electrons occupying nearby charge traps and/or QDs, which are also responsible for spectral wandering.

In III–V semiconductor QDs the nuclear spin bath has a mesoscopic character, limiting electron spin-echo coherence time T_2 to ~1 μs for InGaAs/GaAs [48] and ~30 μs for GaAs/AlGaAs QDs [49]. In group-IV semiconductor qubits electron spin T_2 can be increased via isotope purification by at least 3 orders of magnitude [50]—extension of this approach to II–VI semiconductors may thus lead to optically active QDs with millisecond-range electron spin coherence.

Even more attractive is development of QDs where just a few nuclear spins are used for processing and storage of quantum states. Demonstration of fast (∼1 ms) initialization, long (≳1 s) persistence, and radio frequency manipulation of the nuclei in CdTe QDs is the first step to realizing these concepts. Further progress would require controlling the charge state of the dot and its environment (e.g., using gated charge-tunable structures). In this way, inhomogeneous NMR broadening can be overcome, enabling coherent manipulation of the nuclear spins. Strong electron-nuclear interaction (observed as large Knight shifts) and isotope engineering may allow, in principle, coherence transfer between electron and individual nuclear spins. This would make the nuclei of the II–VI QDs a valuable resource, allowing implementation of the hybrid electron-nuclear spin quantum registers [14], which are not feasible in III–V quantum dots.

This work was supported by the EPSRC Programme Grant No. EP/N031776/1. E. A. C. was supported by a University Research Fellowship from the Royal Society. J. K., W. P., and K. S. were supported by the Polish National Science Center (Grants No. DEC-2015/16/T/ST3/00371 and No. DEC-2015/18/E/ST3/00559).

*gragunathan1@sheffield.ac.uk
†Jakub.Kobak@fuw.edu.pl
‡e.chekhovich@sheffield.ac.uk

[1] H. J. Kimble, Nature (London) **453**, 1023 (2008).
[2] N. Somaschi, V. Giesz, L. De Santis, J. C. Loredo, M. P. Almeida, G. Hornecker, S. L. Portalupi, T. Grange, C. Anton, J. Demory, C. Gomez, I. Sagnes, N. D. Lanzillotti-Kimura, A. Lemaitre, A. Auffeves, A. G. White, L. Lanco, and P. Senellart, Nat. Photonics **10**, 340 (2016).
[3] X. Ding, Y. He, Z.-C. Duan, N. Gregersen, M.-C. Chen, S. Unsleber, S. Maier, C. Schneider, M. Kamp, S. Höfling, C.-Y. Lu, and J.-W. Pan, Phys. Rev. Lett. **116**, 020401 (2016).
[4] R. Stockill, M. J. Stanley, L. Huthmacher, E. Clarke, M. Hugues, A. J. Miller, C. Matthiesen, C. Le Gall, and M. Atatüre, Phys. Rev. Lett. **119**, 010503 (2017).
[5] D. Loss and D. P. DiVincenzo, Phys. Rev. A **57**, 120 (1998).
[6] B. Urbaszek, X. Marie, T. Amand, O. Krebs, P. Voisin, P. Maletinsky, A. Högele, and A. Imamoglu, Rev. Mod. Phys. **85**, 79 (2013).
[7] E. A. Chekhovich, M. N. Makhonin, A. I. Tartakovskii, A. Yacoby, H. Bluhm, K. C. Nowack, and L. M. K. Vandersypen, Nat. Mater. **12**, 494 (2013).
[8] L. Childress, M. V. Gurudev Dutt, J. M. Taylor, A. S. Zibrov, F. Jelezko, J. Wrachtrup, P. R. Hemmer, and M. D. Lukin, Science **314**, 281 (2006).
[9] J. J. Pla, K. Y. Tan, J. P. Dehollain, W. H. Lim, J. J. L. Morton, D. N. Jamieson, A. S. Dzurak, and A. Morello, Nature (London) **489**, 541 (2012).
[10] I. A. Akimov, D. H. Feng, and F. Henneberger, Phys. Rev. Lett. **97**, 056602 (2006).
[11] D. H. Feng, I. A. Akimov, and F. Henneberger, Phys. Rev. Lett. **99**, 036604 (2007).
[12] J. Kim, J. Puls, Y. S. Chen, G. Bacher, and F. Henneberger, Appl. Phys. Lett. **96**, 151908 (2010).
[13] C. Le Gall, A. Brunetti, H. Boukari, and L. Besombes, Phys. Rev. B **85**, 195312 (2012).
[14] M. V. G. Dutt, L. Childress, L. Jiang, E. Togan, J. Maze, F. Jelezko, A. S. Zibrov, P. R. Hemmer, and M. D. Lukin, Science **316**, 1312 (2007).
[15] F. Tinjod, B. Gilles, S. Moehl, K. Kheng, and H. Mariette, Appl. Phys. Lett. **82**, 4340 (2003).
[16] J. Kobak, J.-G. Rousset, R. Rudniewski, E. Janik, T. Slupinski, P. Kossacki, A. Golnik, and W. Pacuski, J. Cryst. Growth **378**, 274 (2013).
[17] See Supplemental Material at http://link.aps.org/supplemental/10.1103/PhysRevLett.122.096801 for additional results and discussion, which includes Refs. [18–32].
[18] J. Suffczyński, T. Kazimierczuk, M. Goryca, B. Piechal, A. Trajnerowicz, K. Kowalik, P. Kossacki, A. Golnik, K. P. Korona, M. Nawrocki, J. A. Gaj, and G. Karczewski, Phys. Rev. B **74**, 085319 (2006).
[19] T. Smoleński, T. Kazimierczuk, M. Goryca, T. Jakubczyk, L. Kłopotowski, L. Cywiński, P. Wojnar, A. Golnik, and P. Kossacki, Phys. Rev. B **86**, 241305 (2012).
[20] M. Bayer, G. Ortner, O. Stern, A. Kuther, A. A. Gorbunov, A. Forchel, P. Hawrylak, S. Fafard, K. Hinzer, T. L. Reinecke, S. N. Walck, J. P. Reithmaier, F. Klopf, and F. Schäfer, Phys. Rev. B **65**, 195315 (2002).
[21] M. Bayer, O. Stern, A. Kuther, and A. Forchel, Phys. Rev. B **61**, 7273 (2000).
[22] G. Schmieder, W. Maier, L. Pu-Lin, and C. Klingshirn, J. Lumin. **28**, 357 (1983).
[23] Y. Léger, L. Besombes, L. Maingault, and H. Mariette, Phys. Rev. B **76**, 045331 (2007).
[24] C. P. Slichter, *Principles of Magnetic Resonance*, 3rd ed. (Springer, New York, 1996).
[25] E. A. Chekhovich, I. M. Griffiths, M. S. Skolnick, H. Huang, S. F. Covre da Silva, X. Yuan, and A. Rastelli, Phys. Rev. B **97**, 235311 (2018).
[26] S. A. Blanton, M. A. Hines, and P. Guyot-Sionnest, Appl. Phys. Lett. **69**, 3905 (1996).
[27] J. Houel, A. V. Kuhlmann, L. Greuter, F. Xue, M. Poggio, B. D. Gerardot, P. A. Dalgarno, A. Badolato, P. M. Petroff, A. Ludwig, D. Reuter, A. D. Wieck, and R. J. Warburton, Phys. Rev. Lett. **108**, 107401 (2012).
[28] A. Abragam, *The Principles of Nuclear Magnetism* (Oxford University Press, London, 1961).
[29] I. J. Lowe and S. Gade, Phys. Rev. **156**, 817 (1967).
[30] E. R. Butkevich and R. K. Sabirov, Phys. Status Solidi B **146**, 683 (1988).
[31] E. A. Chekhovich, K. V. Kavokin, J. Puebla, A. B. Krysa, M. Hopkinson, A. D. Andreev, A. M. Sanchez, R. Beanland, M. S. Skolnick, and A. I. Tartakovskii, Nat. Nanotechnol. **7**, 646 (2012).
[32] R. K. Harris, E. D. Becker, S. M. Cabral De Menezes, R. Goodfellow, and P. Granger, Concepts Magn. Reson. **14**, 326 (2002).
[33] D. Gammon, A. L. Efros, T. A. Kennedy, M. Rosen, D. S. Katzer, D. Park, S. W. Brown, V. L. Korenev, and I. A. Merkulov, Phys. Rev. Lett. **86**, 5176 (2001).

[34] E. A. Chekhovich, A. B. Krysa, M. S. Skolnick, and A. I. Tartakovskii, Phys. Rev. B **83**, 125318 (2011).
[35] J. Puebla, E. A. Chekhovich, M. Hopkinson, P. Senellart, A. Lemaître, M. S. Skolnick, and A. I. Tartakovskii, Phys. Rev. B **88**, 045306 (2013).
[36] A. Ulhaq, Q. Duan, E. Zallo, F. Ding, O. G. Schmidt, A. I. Tartakovskii, M. S. Skolnick, and E. A. Chekhovich, Phys. Rev. B **93**, 165306 (2016).
[37] E. A. Chekhovich, M. N. Makhonin, J. Skiba-Szymanska, A. B. Krysa, V. D. Kulakovskii, M. S. Skolnick, and A. I. Tartakovskii, Phys. Rev. B **81**, 245308 (2010).
[38] B. Urbaszek, P.-F. Braun, T. Amand, O. Krebs, T. Belhadj, A. Lemaítre, P. Voisin, and X. Marie, Phys. Rev. B **76**, 201301 (2007).
[39] A. E. Nikolaenko, E. A. Chekhovich, M. N. Makhonin, I. W. Drouzas, A. B. Van'kov, J. Skiba-Szymanska, M. S. Skolnick, P. Senellart, D. Martrou, A. Lemaître, and A. I. Tartakovskii, Phys. Rev. B **79**, 081303 (2009).
[40] T. Belhadj, T. Kuroda, C.-M. Simon, T. Amand, T. Mano, K. Sakoda, N. Koguchi, X. Marie, and B. Urbaszek, Phys. Rev. B **78**, 205325 (2008).
[41] P. Maletinsky, A. Badolato, and A. Imamoglu, Phys. Rev. Lett. **99**, 056804 (2007).
[42] C. Latta, A. Srivastava, and A. Imamoglu, Phys. Rev. Lett. **107**, 167401 (2011).
[43] C. W. Lai, P. Maletinsky, A. Badolato, and A. Imamoglu, Phys. Rev. Lett. **96**, 167403 (2006).
[44] E. A. Chekhovich, A. Ulhaq, E. Zallo, F. Ding, O. G. Schmidt, and M. S. Skolnick, Nat. Mater. **16**, 982 (2017).
[45] A. Nakamura, D. Paget, C. Hermann, C. Weisbuch, G. Lampel, and B. Cavenett, Solid State Commun. **30**, 411 (1979).
[46] T. Auer, R. Oulton, A. Bauschulte, D. R. Yakovlev, M. Bayer, S. Y. Verbin, R. V. Cherbunin, D. Reuter, and A. D. Wieck, Phys. Rev. B **80**, 205303 (2009).
[47] Note that the broad background is also observed for QD1 in Fig. 3(a), though to a smaller extent, implying a smaller fraction of time in an electron-charged state.
[48] A. Bechtold, D. Rauch, F. Li, T. Simmet, P.-L. Ardelt, A. Regler, K. Muller, N. A. Sinitsyn, and J. J. Finley, Nat. Phys. **11**, 1005 (2015).
[49] H. Bluhm, S. Foletti, I. Neder, M. Rudner, D. Mahalu, V. Umansky, and A. Yacoby, Nat. Phys. **7**, 109 (2011).
[50] E. Abe, A. M. Tyryshkin, S. Tojo, J. J. L. Morton, W. M. Witzel, A. Fujimoto, J. W. Ager, E. E. Haller, J. Isoya, S. A. Lyon, M. L. W. Thewalt, and K. M. Itoh, Phys. Rev. B **82**, 121201 (2010).